

SENSITIVITY MAP GENERATION FOR CONDUCTING STRATEGY IN ELECTRICAL RESISTANCE TOMOGRAPHY

Suzanna Ridzuan Aw^a, Ruzairi Abdul Rahim^{b*}, Fazlul Rahman Mohd Yunus^b, Mohd Hafiz Fazalul Rahiman^c, Yasmin Abdul Wahab^d, Mohd Badril Nor Shah^e, Jayasuman Pusppanathan^b, Elmy Johana Mohamed^f

^aFaculty of Electrical & Automation Engineering Technology, Terengganu Advance Technical Institute University College (TATIUC), Jalan Panchor, Telok Kalong, 24000, Kemaman, Terengganu, Malaysia

^bProcess Tomography and Instrumentation Engineering Research Group (PROTOM-i), Innovative Engineering Research Alliance, Faculty of Electrical Engineering, Universiti Teknologi Malaysia, 81310 UTM Johor Bahru, Johor, Malaysia

^cSchool of Mechatronic Engineering, Universiti Malaysia Perlis, Pauh Putra Campus, 02600 Arau, Perlis, Malaysia

^dDepartment of Instrumentation & Control Engineering (ICE), Faculty of Electrical & Electronics Engineering, Universiti Malaysia Pahang, 26600 Pekan, Pahang, Malaysia

^eUniversiti Teknikal Malaysia, 76100, Melaka, Malaysia

^fDepartment of Mechatronics and Robotics, Faculty of Electrical and Electronic Engineering, Universiti Tun Hussein Onn Malaysia, 86400, Johor, Malaysia

Article history

Received

28 June 2015

Received in revised form

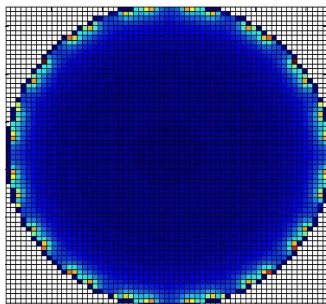
1 September 2015

Accepted

15 October 2015

*Corresponding author
ruzairi@fke.utm.my

Graphical abstract



Abstract

This paper presents the sensitivity map generation of Electrical Resistance Tomography (ERT) for a system using conducting vessel pipe. A finite element model software using 2D COMSOL model consisting of 16 electrodes were attached invasively in a stainless steel pipe to solve for the forward problem. The conducting boundary approach was applied to the system to avoid the grounding effect.

Keywords: Conducting boundary strategy, COMSOL, electrical resistance tomography, sensitivity map

© 2015 Penerbit UTM Press. All rights reserved

1.0 INTRODUCTION

Electrical Resistance Tomography (ERT) has become a promising technique in monitoring and analysing various industrial flows due to its diverse advantages, such as high speed, low cost, suitability for various sizes of pipes and vessels, having no radiation hazard, and being non-intrusive [1-3]. It provides the cross sectional images of conductivity distribution within its sensing region. For a system employing ERT on a metallic or conducting vessel pipe, the electrodes need to be insulated from the pipe wall. In addition, the conducting boundary strategy needs to be applied to overcome the grounding effect [4, 5].

The sensing field of ERT system is spread over the entire volume due to the "soft-field" characteristics [6-8]. The paths of electric currents in ERT are not straight lines. Current diffuses all over the target, and the current distribution in the material depends on the internal conductivity distribution $\sigma = \sigma(r)$ [9]. The image reconstruction problem of conductivity distribution in ERT is an ill-posed and ill-conditioned inverse problem. To solve for the inverse problem, a forward model which relates to the dependency between conductivity distribution and boundary voltages need to be solved first. Since the ERT model is nonlinear and difficult to be solved analytically, the finite element method (FEM) is preferable to solve for the forward model. From the solution, the data is interpolated to generate the sensitivity distribution and then be used to solve the inverse problem later.

This paper discussed the generation of sensitivity distribution for ERT system employing a conducting vessel pipe. Finite element method using COMSOL software is implemented to solve for the forward model. The data obtained were then interpolated in the MATLAB to obtain the sensitivity distribution for every possible injection-measurement electrode pair.

2.0 ERT FOR CONDUCTING VESSEL

Before applying ERT to an electrically-conducting vessel, an electrical path passing through the vessel wall must be taken into consideration. The adjacent strategy is unsuitable for application to the conducting vessel since much of the electrical current from the injection electrode would travel to ground through the wall material rather than through the multiphase mixture, greatly reducing sensitivity. This is called the grounding effect of the vessel. One possible method of accounting for the conducting vessel wall is to use the wall itself as the ground electrode [10]. Conducting boundary strategy, as in Figure 1, has been proposed and developed by [4] for the conducting vessel wall to overcome the grounding effect. The strategy considers each electrode acting sequentially as a current source whilst the whole of the metallic vessel behaves as a grounded current sink. In this strategy, all voltage measurements are referenced to the same earth potential of the conducting boundary.

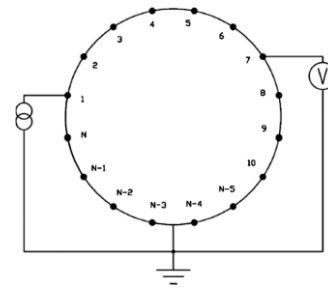


Figure 1 Conducting Boundary Strategy [11]

2.1 Forward Problem

ERT belongs to a class of diffuse tomography modalities since the paths of electric currents are not straight lines. Accurate modelling of the measurements and prior information of the target distribution is required in solving the inverse problem [7].

Forward model will be used later to solve the inverse problem which is the reconstruction problem in ERT. The so far most accurate model for ERT measurements is the complete electrode model introduced by Cheng et al. [12]. The complete electrode model consists of the following partial differential equation and the boundary conditions

$$\nabla \cdot (\sigma \nabla u) = 0, r \in \Omega \quad (1)$$

$$\int_{e_l} \sigma \frac{\partial u}{\partial n} dS = I_l, r \in e_l, l = 1, \dots, L \quad (2)$$

$$\sigma \frac{\partial u}{\partial n} = 0, r \in \partial\Omega \setminus \cup_{l=1}^L e_l \quad (3)$$

$$u + z_l \sigma \frac{\partial u}{\partial n} = U_l, r \in e_l, l = 1, \dots, L \quad (4)$$

where;

Ω = computational domain

$\sigma = \sigma(r)$ = conductivity distribution

$u = u(r)$ = electric potential inside Ω

U_l = potential on l th electrode

I_l = current on l th electrode

z_l = contact impedance between the l th electrode and the object

n = outward unit normal

In addition, the Kirchoff's current Law

$$\sum_{l=1}^L I_l = 0 \quad (5)$$

must be fulfilled, and the potential reference level has to be fixed, for example by writing

$$\sum_{l=1}^L U_l = 0 \quad (6)$$

The solution of the ERT forward problem is by computing electrode potentials U_l given the conductivity distribution and the electrode currents I_l is

obtained by solving the partial differential equation (1) with conditions (2)–(6). The system (1)–(6) has a unique solution which can be approximated by using finite element method (FEM) [7]. The FE approximation of the model results the following form

$$V = R(\sigma, z) + v \tag{7}$$

where;

V = voltage observations (potential on l th electrode, U_l)

$R(\sigma, z)$ = mapping from the conductivity distribution σ and the contact impedance z to the electrode voltages

v = measurement noise vector

2.2 Sensitivity Distribution using Conducting Strategy

The sensitivity theorem or lead theorem which analysed the boundary mutual impedance experienced by the changes of conductivity within the sensing region has been introduced by Geselowitz and later refined by Lehr. It is based on the Green's theorem and the divergence theorem [13]. By adapting the two theorems to a conducting volume as shown in Figure 1, the reciprocity theorem (Equation 8) and lead theorem of mutual impedance Z (Equation 9) can be deduced as [14]:

$$I_\psi \psi_{AB} = I_\phi \phi_{CD} \tag{8}$$

$$Z = \phi_{CD} / I_\phi = \psi_{AB} / I_\psi \tag{9}$$

where ψ_{AB} and ϕ_{CD} are the voltage potentials measured between terminal AB and CD due to the injection currents I_ψ and I_ϕ respectively.

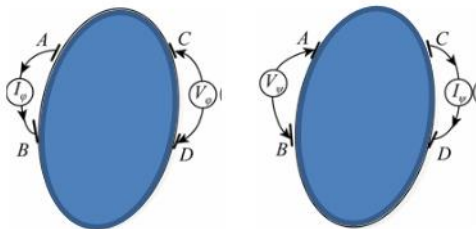


Figure 2 Illustration of Current Injection and Potential Measurement for Mutual Impedance Relation between Terminal AB and CD [15]

From the divergence and reciprocity theorem, Geselowitz and Lehr derived a relationship between the mutual impedance changes, ΔZ and the conductivity changes, $\Delta\sigma$ [16]:

$$\Delta Z = \frac{\Delta\phi_{CD}}{I_\phi} = - \int_v \Delta\sigma \frac{\nabla\phi}{I_\phi} \cdot \frac{\nabla\psi}{I_\psi} dv \tag{10}$$

Solving for Eq. 1, the sensitivity theorem to solve the inverse problem of ERT can be simplified to:

$$S_{ij} = \frac{\Delta R}{\Delta\sigma} = - \int_v \frac{\nabla\phi_i}{I_i} \cdot \frac{\nabla\phi_j}{I_j} dv \tag{11}$$

where:

S_{ij} : sensitivity distribution when the i -th and j -th electrode pair is in excitation and measurement respectively.

R : mutual resistance that is a special case of mutual impedance, Z .

ϕ_i : potential distributions within the medium when the i -th electrode is excited by current I_i .

ϕ_j : potential distributions within the medium when the j -th electrode is excited by current I_j .

Assuming that the conductivity distribution is composed of k small uniform pixels, the sensitivity coefficient of each pixel can be deduced as [15]

$$s_{i,j}(k) = - \int_{\Omega_k} \frac{\nabla\phi_{ik}}{I_i} \cdot \frac{\nabla\phi_{jk}}{I_j} d\Omega_k \tag{12}$$

where:

Ω_k : discrete 2D area of the k -th pixel,

$s_{i,j}(k)$: sensitivity coefficient at the k -th pixel when the i -th and j -th electrode pairs are in excitation and measurement respectively,

ϕ_{ik} : potential distributions at the k -th pixel when the i -th electrode is excited by current I_i .

ϕ_{jk} : potential distributions at the k -th pixel when the j -th electrode is excited by current I_j .

The sensitivity matrix can then be expressed by [15]

$$S = \begin{bmatrix} s_{1,2}(1) & s_{1,2}(2) & \dots & s_{1,2}(k) & \dots & s_{1,2}(M) \\ s_{1,3}(1) & s_{1,3}(2) & \dots & s_{1,3}(k) & \dots & s_{1,3}(M) \\ \vdots & \vdots & \ddots & \vdots & \ddots & \vdots \\ s_{i,j}(1) & s_{i,j}(2) & \dots & s_{i,j}(k) & \dots & s_{i,j}(M) \\ \vdots & \vdots & \ddots & \vdots & \ddots & \vdots \\ s_{n-2n}(1) & s_{n-2n}(2) & \dots & s_{n-2n}(k) & \dots & s_{n-2n}(M) \end{bmatrix} \tag{13}$$

The sensitivity theorem is also applicable to the conducting vessel because the electrical field within the vessel still obeys Greens' and the reciprocity theorem. The number of unique measurements, N , in the conducting boundary strategy is $n(n - 1)/2$ where n is the number of electrodes.

3.0 METHODOLOGY

The sensitivity distribution of a homogeneous conductivity medium can be acquired by solving the forward model using both analytical and numerical method. Since it is difficult to obtain the analytical solutions of the equation, the numerical solvers, i.e., the finite element methods (FEM) are more preferable and the most commonly used methods to solve the forward problem. COMSOL Multiphysics 4.2, a finite

element analysis tool has been utilized in this work to solve for the forward problem of an ERT system of a conducting vessel pipe.

COMSOL Multiphysics software is a powerful interactive environment for modelling and solving all kinds of scientific and engineering problems. It offers a complete and integrated modelling environment for creating, analysing and visualizing multiphysics models. The software internally compiles a set of equations representing the entire model. The model was created by defining the relevant physical quantities such as material properties, loads, constraints, sources, and fluxes rather than outlining the underlying equations.

Before creating the model using COMSOL, it was decided that a flexible circuit board as the electrode would be used. It is to be noted that metal electrodes for electrically-conducting (metallic) column differ slightly from a non-conducting (insulating) column in which the electrodes need to be insulated from the conducting column. A design was proposed for the electrode fabrication to be implemented in ERT system deploying conducting vessel. Figure 2 shows the design of electrode fabrication using flexible circuit board of the proposed system.

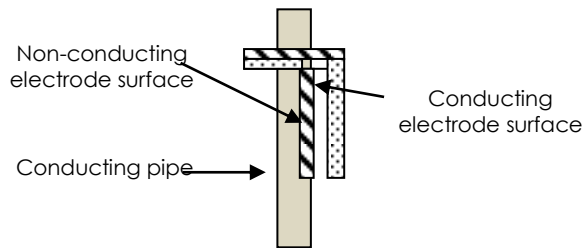


Figure 3 Electrode Fabrication using flexible circuit board

Sixteen rectangular electrodes of 12 mm x 100 mm were implemented. The electrodes were mounted at the center of the stainless steel column and evenly spaced along the circumference. The system is modelled in 2D using COMSOL. The parameters used throughout the simulation are shown in Table 1. It is assumed that the electrodes make electrical contact with the fluid inside the column but do not affect the normal mass transfer within the system.

Table 1 Simulation parameters with COMSOL 4.2a

Parameter	Value
Column Inner radius	50 mm
Column Outer radius	51 mm
Column Height	300 mm
Number of electrodes (N)	16
Electrode's material	Gold
Insulator's material	FR4
Electrode's height (h)	100 mm
Electrode's width (w)	12 mm
Current excitation	20 mA
σ_{water}	$8.3 \times 10^{-3} \text{ S/m}$

A 2D space dimension, **Electric Currents** of physics interface under the AC/DC branch and stationary study were selected respectively for the COMSOL simulation. After that, the following steps were taken to solve the forward problem and generating the sensitivity matrix:

i. Create a physical model using available geometries:

A 2D physical model has been developed such that it mimics a real system. Sixteen electrodes that were insulated from the column wall were placed equidistantly inside the column.

ii. Define materials for each domain in the created model:

The materials for each related domain in the model were defined such that it also resembles a real system. The column itself was defined as stainless steel material and the main medium inside the column was the tap water with a conductivity of 8.3 mS/m. The electrodes implemented are from the flexible gold coated printed circuit board (PCB). FR4 material is chosen as the material for the insulating part of the electrodes.

iii. Assign relevant physics interface and define boundary and initial conditions that describe real experiment setup:

"Electric Currents" interface was chosen since it would produce an electrical field and has the electrical potential distribution required for the analysis. It also contained the equations, boundary conditions, and current sources for modelling electric currents in conductive media, solving the electric potential.

To overcome the grounding effect of the vessel, a conducting boundary strategy was implemented on the model. The strategy considered that each electrode would act sequentially as a current source whilst the whole of the conducting vessel behaved as a grounded current sink. A constant current of 10 mA was injected at source electrode initially at e_1 . In this strategy, all the voltage measurements were referenced to the same earth potential of the conducting boundary which is the pipe itself [17]. The cross section view of the COMSOL model is shown in Figure 3.

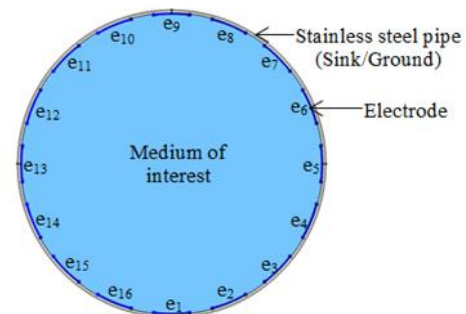


Figure 4 2D COMSOL ERT Model using Metal Pipe

iv. Mesh the model

In a simulation process, meshing geometry can be crucial in obtaining the best results in faster way. Extra fine meshing under meshing physics controlled setting is chosen since denser meshing would provide a more reliable finite element method (FEM) simulation.

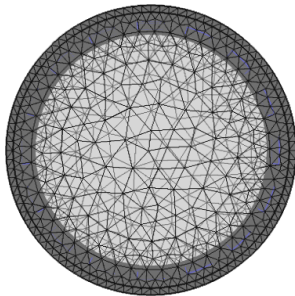


Figure 5 Extra Fine Meshing using COMSOL Multiphysics

v. Run the study:

The investigated model is simulated using the default solver under stationary study. In applying the stationary solver, it is assumed that the load and deformation do not vary in time. The physic interface chosen earlier solves the ERT forward problem which computes the electrode potentials given the conductivity distribution and the electrode. It numerically solves the partial differential equation (PDE) and boundary condition.

vi. Pre-process the data for result analysis

Last but not least, the results are pre-processed and interpolated to generate the sensitivity matrix. The medium of interest is subdivided into a number of uniform square sub-domains that serve as pixels in the reconstructed images. Here, 64 x 64 pixels which equals to 4096 pixels is implemented as in Figure 6. At this stage, the electric field, E data were exported elsewhere.

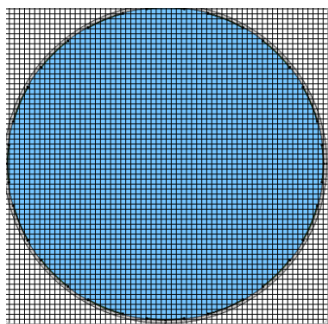


Figure 6 64 x 64 Pixel

Then, the steps were repeated for other source injection to obtain the electric field distribution. The electric potential, φ and the electric field distribution, E is govern by equation:

$$-\nabla\varphi = E \tag{14}$$

Thus, Equation (13) that denotes the sensitivity of electrode pair's i - j (i for excitation and j for measurement) to the conductivity change in a pixel at position k -th can be rewritten as:

$$s_{i,j}(k) = \int_{\Omega_k} (E_{ik}/I_i) \cdot (E_{jk}/I_j) d\Omega_k \tag{15}$$

where E_{ik} and E_{jk} are the electric field strength at k -th pixel when the i -th and j -th electrode pairs are injected with currents I_i and I_j respectively in turn[18]. Practically, it is assumed that the electric field is the same at every point of the area Ω_k since the pixels are so small. Assuming a unit current, Equation (15) can be deduced to

$$s_{i,j}(k) = E_{ikc} \cdot E_{jkc} A_{\Omega_k} \tag{16}$$

where E_{ikc} and E_{jkc} are the electric field intensities at the centre of k -th pixel when the i -th electrode pair is in excitation mode and j -th electrode pair is measurement mode. A_{Ω_k} is the area of the k -th pixel.

Last but not least, the sensitivity coefficient of each pixel is obtained. The sensitivity coefficient for each electrode pair at a spatial location k -th is obtained by dot product the two electric fields. The two electric fields are from the post-processing step vi described above. In this paper, the sensitivity map as in Figure 6 is used since it represents the sensitivity matrix [8].

From the reciprocity theorem, for 16 electrodes system employing the conducting boundary strategy, a total of 120 sensitivity map will be produced. It represents all possible injection pair ($e_i e_j$) for the strategy, where e_i denotes the excitation source electrode and e_j denotes the receiver, measurement electrode. This is shown in Table 2 where only the "peach" color cells not marked by x were considered.

Table 2 Independent Measurement Strategy for Conducting Boundary

Receiver Source	e1	e2	e3	e4	e5	e6	e7	e8	e9	e10	e11	e12	e13	e14	e15	e16	No. of measurement
e1	x																15
e2	x	x															14
e3	x	x	x														13
e4	x	x	x	x													12
e5	x	x	x	x	x												11
e6	x	x	x	x	x	x											10
e7	x	x	x	x	x	x	x										9
e8	x	x	x	x	x	x	x	x									8
e9	x	x	x	x	x	x	x	x	x								7
e10	x	x	x	x	x	x	x	x	x	x							6
e11	x	x	x	x	x	x	x	x	x	x	x						5
e12	x	x	x	x	x	x	x	x	x	x	x	x					4
e13	x	x	x	x	x	x	x	x	x	x	x	x	x				3
e14	x	x	x	x	x	x	x	x	x	x	x	x	x	x			2
e15	x	x	x	x	x	x	x	x	x	x	x	x	x	x	x		1
e16	x	x	x	x	x	x	x	x	x	x	x	x	x	x	x	x	0
Total Measurements																	120

4.0 RESULTS AND DISCUSSIONS

The sensitivity map for different configurations of electrode excitation of the ERT system that was fitted with 16 electrodes on a stainless steel pipe modelled in COMSOL are illustrated in Figure 7. Figure 7a represents the sensitivity distribution of e_1e_9 that is when electrode e_1 is in excitation and e_9 in measurement. Figure 7b to 7e represent the injection pair between electrode e_2 and e_{14} , e_5 and e_9 , e_7 and e_{10} , e_{11} and e_{15} respectively. The combination of all independent projection electrode pair configurations is shown in Figure 7f. It is also known as the weight balance map. All other sensitivity distribution for opposite measurement will resemble the result in Figure 7a whilst the sensitivity for a 90° measurement electrode pair will resemble the pattern in Figure 7c. From the results, it is observed that the sensitivity field is non-uniformly distributed over the medium of interest. The sensitivity is higher within the area close to both excitation and measurement electrode pair. When it is away from the active injection electrode pair, the sensitivity is lower.

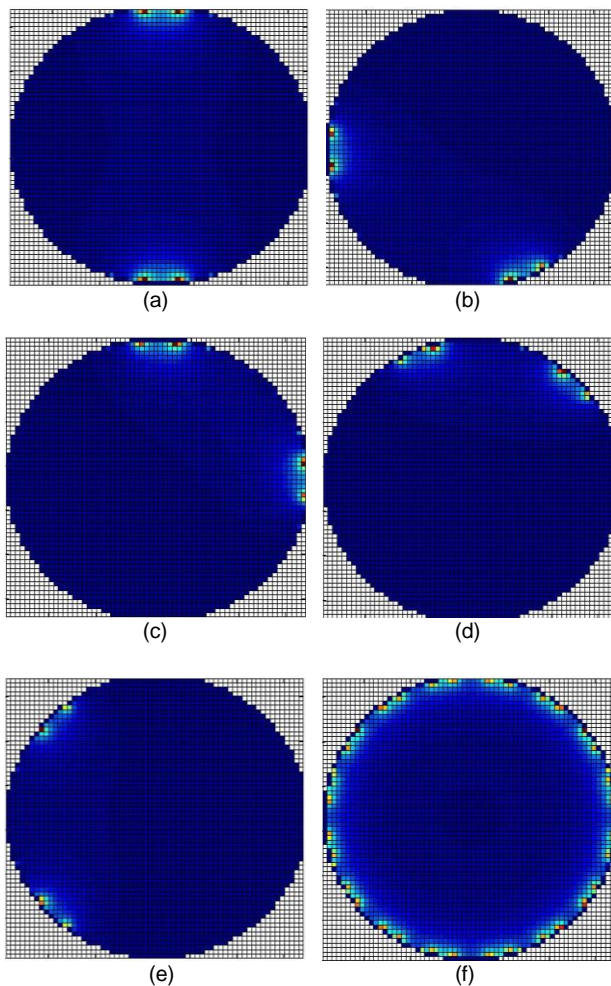


Figure 7 Sensitivity Map Distribution of:

- (a) electrode 1 and 9 (b) electrode 2 and 13
 (c) electrode 5 and 9 (d) electrode 7 and 10
 (e) electrode 11 and 15 (f) total projection

5.0 CONCLUSION

Linearization remains a widespread choice in ERT image reconstruction. Even it could not provide an accurate image due to its linear approach; it does provide a fast on-line view for initial visualization. Generating the sensitivity distribution or also known as the sensitivity map of a homogeneous medium is a very important step in linearization method. A correct sensitivity map is crucial to solve for the inverse problem in producing a correct image reconstruction. Before solving for the dot product of two electric fields for any electrode pair projection, the forward problem of the system need to be solved first. COMSOL has proven to be a powerful tool of numerical solution to solve for the forward model.

Acknowledgement

The authors would like to acknowledge the Research University grant (08h31, PY/2015/04458, PY/2015/ 04567) for funding the IWMYCT conference cost. Authors are also grateful to the PROTOM Research Group UTM and for the financial support from MyBrain15 Programme and TATI University College.

References

- [1] H. Jin, S. Yang, G. He, M. Wang, and R. A. Williams. 2010. The Effect Of Gas-Liquid Counter-Current Operation On Gas Hold-Up In Bubble Columns Using Electrical Resistance Tomography. *Journal of Chemical Technology and Biotechnology*. 85: 1278-1283.
- [2] Y. Xu, H. Wang, Z. Cui, and F. Dong. 2009. Application of Electrical Resistance Tomography For Slug Flow Measurement In Gas/Liquid Flow Of Horizontal Pipe. In *2009 IEEE International Workshop on Imaging Systems and Techniques, IST 2009, May 11, 2009-May 12, 2009, Hong Kong, China*. 319-323.
- [3] T. Dyakowski, L. F. C. Jeanmeure, and A. J. Jaworski. 2000. Applications of Electrical Tomography For Gas-Solids And Liquid-Solids Flows—A Review. *Powder Technology*. 112: 174-192.
- [4] M. Wang, F. J. Dickin, and R. A. Williams. 1994. Electrical Resistance Tomography Of Metal Walled Vessels And Pipelines. *Electronics Letters*. 30: 771-773.
- [5] S. R. Aw, R. A. Rahim, M. H. F. Rahiman, F. R. M. Yunus, and C. L. Goh. 2014. Electrical Resistance Tomography: A Review Of The Application Of Conducting Vessel Walls. *Powder Technology*. 254: 256-264.
- [6] W. R. Fan and H. X. Wang. 2010. Maximum Entropy Regularization Method For Electrical Impedance Tomography Combined With A Normalized Sensitivity Map. *Flow Measurement and Instrumentation*. 21: 277-283.
- [7] A. Seppanen, K. Karhunen, A. Lehtikoinen, J. P. Kaipio, and P. J. M. Monteiro. 2009. Electrical Resistance Tomography Imaging Of Concrete. In *2nd International Conference on Concrete Repair, Rehabilitation and Retrofitting, ICCRRR 2008, November 24, 2008-November 26, 2008, Cape Town, South africa*. 231-232.
- [8] K. Yong Song and et al. 2007. Sensitivity Map Generation In Electrical Capacitance Tomography Using Mixed Normalization Models. *Measurement Science and Technology*. 18: 2092.
- [9] K. Karhunen, A. Seppanen, A. Lehtikoinen, J. Blunt, J. P. Kaipio, and P. J. M. Monteiro. 2010. Electrical Resistance

- Tomography For Assessment Of Cracks In Concrete. *ACI Materials Journal*. 107: 523-531.
- [10] S. G. Liter, J. R. Torczynski, K. A. Shollenberger, and S. L. Ceccio. 2002. Electrical-Impedance Tomography for Opaque Multiphase Flows in Metallic (Electrically-Conducting) Vessels. Sandia National Labs, Albuquerque, NM (US); Sandia National Labs., Livermore, CA (US).
- [11] B. D. Grieve. 2002. On-line Electrical Impedance Tomography for Industrial Batch Processing. Degree of Doctor of Philosophy, Department of Chemical Engineering, UMIST Manchester, UK.
- [12] K. S. Cheng, D. Isaacson, J. C. Newell, and D. G. Gisser. 1989. Electrode Models For Electric Current Computed Tomography. *IEEE Transactions on Biomedical Engineering*. 36: 918-924.
- [13] M. Wang, F. J. Dickin, and R. Mann. 1999. Electrical Resistance Tomographic Sensing Systems For Industrial Applications. *Chemical Engineering Communications*. 175: 49-70.
- [14] S. Huang, Z. Wang, and Y. Jin. 1999. Studies on Gas-Solid-Solid Circulating Fluidized-Bed Reactors. *Chemical Engineering Science*. 54: 2067-2075.
- [15] H. Zhou, L. Xu, Z. Cao, J. Hu, and X. Liu. 2012. Image Reconstruction For Invasive ERT In Vertical Oil Well Logging. *Chinese Journal of Chemical Engineering*. 20: 319-328.
- [16] J. Lehr. 1972. A Vector Derivation Useful in Impedance Plethysmographic Field Calculations. *Biomedical Engineering, IEEE Transactions on*. BME-19: 156-157.
- [17] J. L. Davidson, L. S. Ruffino, D. R. Stephenson, R. Mann, B. D. Grieve, and T. A. York. 2004. Three-dimensional Electrical Impedance Tomography Applied To A Metal-Walled Filtration Test Platform. *Measurement Science and Technology*. 15: 2263.
- [18] J. Sun and W. Yang. 2014. Evaluation of Fringe Effect Of Electrical Resistance Tomography Sensor. *Measurement*. 53: 145-160.